BILINGUAL PUBLISHING CO.
Pioneer of Global Academics Since 1984

01
2020

Journal of Oncology Research

Volume 2 Issue 1 · January 2020 · ISSN 2630-5267

ISSN 2630-5267 01
9 772630 526205
Price: S$30.00

Volume 2 Issue 1 • January 2020 • ISSN 2630-5267 (Online)

Journal of Oncology Research

BILINGUAL PUBLISHING CO.
Pioneer of Global Academics Since 1984

BILINGUAL PUBLISHING CO.
Pioneer of Global Academics Since 1984

Volume 2 | Issue 1 | January 2020 | Page 1-15
Journal of Oncology Research

Contents

Article

Review

BILINGUAL PUBLISHING CO.
Pioneer of Global Academics Since 1984

Journal of Oncology Research
https://ojs.bilpublishing.com/index.php/jor

ARTICLE

Associations between Body Mass Index and Breast Cancer Markers

Ishita Saha[1] Poonam Singh[2] Sunit Kumar Medda[3] Rabindra Nath Das[4*]

1. Department of Physiology, Calcutta Medical College and Hospital, Kolkata, W.B., India
2. Department of Statistics, University of Delhi, Delhi, India
3. Kalyani J.N.M. Hospital, Kalyani, Nadia, West Bengal, India
4. Department of Statistics, The University of Burdwan, Burdwan, West Bengal, India

ARTICLE INFO

Article history
Received: 22 April 2020
Accepted: 18 June 2020
Published: 30 June 2020

Keywords:
Adiponectin
Breast cancer biomarkers
BMI
Leptin
Resistin
Joint mean variance modeling

ABSTRACT

Body mass index (BMI) and breast cancer biomarkers (BCBs) such as resistin, leptin adiponectin, monocyte chemoattractant protein-1 (MCP-1) and homeostasis model assessment of insulin resistance (HOMA-IR) are highly associated with each other. The report has focused the inter-relationship between BMI and BCBs based on probabilistic modeling. It has been shown that mean BMI is directly associated with leptin (P<0.0001) and MCP-1 (P=0.0002), while it is inversely associated with adiponectin (P=0.0003), HOMA-IR (P<0.0001), and it is higher for healthy women (P=0.0116) than breast cancer women. In addition, variance of BMI is inversely associated with resistin (P=0.1450). On the other hand, mean MCP-1 is directly associated with BMI (P<0.0001). Mean resistin is directly associated with the interaction effect of BMI and leptin (BMI*Leptin) (P=0.0415), while its variance is directly associated with BMI (P=0.0942), and it is inversely associated with BMI*Adiponectin (P=0.1518). Leptin is directly associated with BMI (P<0.0001). Also adiponectin is inversely associated with BMI (P<0.0001), BMI*Leptin (P=0.1729), while it is directly associated with Age*BMI (P=0.0017) and BMI*Resistin (P=0.0615). It can be concluded that BMI and BCBs are strongly associated with each other. Care should be taken on BMI for breast cancer women.

1. Introduction

BMI has been a fundamental psychosocial issue among human beings for millennia. It is a composite measure of height and weight, which is defined as BMI= Weight(kg) / Height(m^2). An individual fatness index is measured by BMI. It is considered as the risk factor for the growth of many diseases such as breast cancer, diabetes, cardiovascular diseases, etc. [1-5]. In general, BMI less than or equal to 25 kg/m^2 is treated as the normal, otherwise it is considered as obesity.

Excess weight has been associated with a variety of cancers such as postmenopausal breast, colon, renal, esophageal, endometrial etc. The International Research Agency on Cancer has predicted that BMI causes 9% of breast cancer, 25% of renal cancer, 11% of colon cancer, 39% of endometrial cancer, and 37% of esophageal cancer[6]. Calle et al. [7] pointed that BMI was associated with a greater risk of death from 14 cancers such as esophagus, liver, colon and rectum, gallbladder, kidney, pancreas, non-Hodgkin

**Corresponding Author:*
Rabindra Nath Das,
Department of Statistics, The University of Burdwan, Burdwan, West Bengal, India;
Email: rabin.bwn@gmail.com

 DOI: https://doi.org/10.30564/jor.v2i1.2007

lymphoma, stomach, multiple myeloma, breast, prostate, cervix, uterus, and ovary, and it was predicted that BMI may account for 20% of all cancer deaths in women and 14% in men [7].

BMI is a well-known risk factor for postmenopausal breast cancer, whereas debatable outcomes have been presented in premenopausal women [8-10]. A large sample meta-analysis reported an inverse association between BMI and the chance of premenopausal breast cancer [11]. Recently, two large prevention data studies have shown that premenopausal women with higher BMI are at increased risk for growing breast cancer [12,13].

The relationships between BMI and BCBs are still contradictable [8,9,11,14-16]. These can be studied based on statistical modeling of BMI on the BCBs such as leptin, resistin, adiponectin and MCP-1 and other explanatory variables. Again, each BCB should be modeled on BMI and other explanatory variables. The current report focuses the associations between BMI and BCBs based on modeling of BMI, MCP-1, adiponection, resistin, and leptin. For a data set given in [17,18], these models have been studied in [19-23]. From these models, the relationships between BMI and BCBs are reported in the current article.

2. Materials and Methods

2.1 Materials

The data set can be found in the UCI Machine Learning Repository, and its detailed description is given in [17,18]. For immediate using of the covariates in the report, these are restated as BMI (kg/m^2), Age, HOMA-IR, Insulin (μU/mL), Glucose (mg/dL), Adiponectin (μg/mL), Resistin (ng/mL), MCP-1, Leptin(ng/mL), Types of Patient (TYOP) (1=healthy controls; 2=patients).

2.2 Statistical Methods

The considered data set given in [17,18] is a multivariate data set. The interested responses are BMI, resistin, MCP-1, adiponectin, leptin which are all positive continuous heterogeneous and non-normally distributed. These are required to be modeled herein. These can be appropriately modeled using joint generalized linear models (JGLMs) adopting both the Log-normal and Gamma distributions, which are clearly given in [24-26]. Both the JGLMs under the Log-normal and Gamma distributions are very shortly given in recent articles [22-23], which are not reproduced herein. For more discussions on JGLMs, readers can visit [24,25].

2.3 Statistical and Graphical Analysis

For ready reference, first we examine BMI model on age, insulin, glucose, and BCBs. The detailed analysis is given by Das et al. [19]. It is mentioned herein that BMI and BCBs such as MCP-1, resistin, leptin and adiponectin can be modeled adopting JGLMs under both the Log-normal & Gamma distributions [24-26]. Log-normal JGLMs fit of BMI is better than the Gamma fit, which is presented in Table 1, and its fitting diagnostic is revealed in Figure 1. Figure 1(a) displays the absolute residuals plot against the predicted BMI values, which is closely a flat straight line, implying that variance is constant with the running means. Figure 1(b) represents the normal probability plot of the fitted BMI mean Log-normal model in Table 1. No lack of fit is identified in both the figures. So, Log-normal fitted BMI model (Table 1) is an approximate form of its true model. Fitted BMI mean & dispersion models are as follows:

Fitted Log-normal BMI mean ($\hat{Z}$) model (from Table 1) is

$\hat{Z}$ = Log(BMI)= 3.0370 - 0.0421 HOMA-IR + 0.0015 Glucose + 0.0123 Insulin - 0.0068 Adiponectin + 0.0001 MCP-1 + 0.0053 Leptin - 0.0708 TYOP,

and the BMI fitted Log-normal variance ($\hat{\sigma}^2$) model is

$\hat{\sigma}^2$ = exp. (-4.445 - 0.018 Insulin - 0.019 Resistin + 0.015Age).

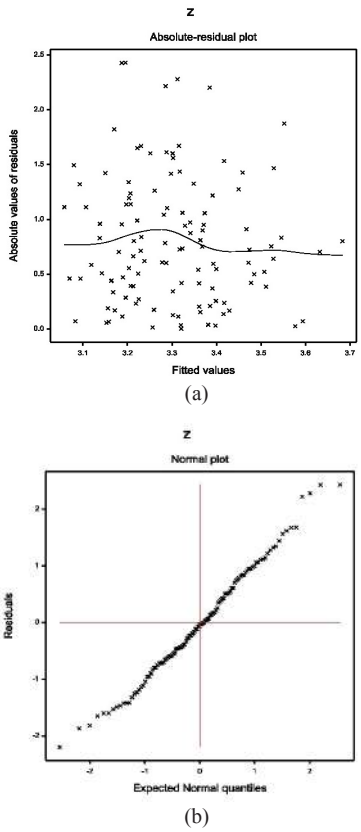

(a)

(b)

Figure 1. For the joint Log-normal BMI fitted models (Table 1), the (a) absolute residuals plot against the fitted values, and (b) the normal probability plot for the mean BMI model

DOI: https://doi.org/10.30564/jor.v2i1.2007

Table 1. Results for mean and dispersion models for BMI from Log-Normal and Gamma fit

Model	Covariates	Log-normal				Gamma			
		Estimate	s.e.	t-value	P-Value	Estimate	s.e.	t-value	P-Value
Mean	Constant	3.0370	0.08363	36.3122	<0.0001	3.0460	0.08367	36.4013	<0.0001
	Glucose (x3)	0.0015	0.00084	1.7961	0.0753	0.0016	0.00085	1.8502	0.0670
	Insulin (x4)	0.0123	0.00318	3.8502	0.0002	0.0121	0.00318	3.8281	0.0002
	HOMA-IR (x5)	-0.0421	0.01033	-4.0823	<0.0001	-0.0421	0.01019	-4.1333	<0.0001
	Leptin (x6)	0.0053	0.00063	8.2341	<0.0001	0.0052	0.00065	8.0953	<0.0001
	Adiponectin (x7)	-0.0068	0.00184	-3.7363	0.0003	-0.0068	0.00186	-3.6552	0.0004
	MCP-1 (x9)	0.0001	0.00005	3.8724	0.0002	0.0001	0.00006	3.7272	0.0003
	Patient's typ (Fx10)	-0.0708	0.02758	-2.5681	0.0116	-0.0699	0.02768	-2.5241	0.0130
Dispersion	Constant	-4.445	0.7261	-6.1224	<0.0001	-4.358	0.7167	-6.0821	<0.0001
	Age (x1)	0.015	0.0107	1.3652	0.1751	0.013	0.0108	1.2652	0.2085
	Resistin (x8)	-0.019	0.0132	-1.4683	0.1450	-0.020	0.0134	-1.5082	0.1344
	Insulin (x4)	-0.018	0.0156	-1.1784	0.2413	-0.019	0.0157	-1.2233	0.2239
	AIC= 613.9					AIC=615.062			

Biomarker MCP-1 analysis is given by Kim et al. [20], and for ready reference it is reproduced in Table 2. Fitted MCP-1 mean & dispersion models are as follows:

MCP-1Gamma fitted mean ($\hat{\mu}$) model (from Table 2) is

$\hat{\mu}$ = exp(5.1791 - 0.0265 Insulin + 0.0455 BMI - 0.0192 Leptin + 0.0220 Resistin + 0.0009 Insulin*Leptin),

and MCP-1Gamma fitted dispersion ($\hat{\sigma}^2$) model (from Table 2) is

$\hat{\sigma}^2$ = exp(0.7374 - 0.0868 Insulin - 0.0293 Age + 0.0051 Age*Insulin + 0.0053 Glucose - 0.8286 HOMA-IR - 0.0997 Leptin - 0.0405 Resistin + 0.0007 Glucose*Leptin + 0.0010 Leptin*Resistin).

Table 2. Results for mean & dispersion models for MCP-1 from Log-Normal and Gamma fit

Model	**Covariate**	**Gamma Model**				**Log-normal Model**			
		estimate	**s.e.**	**t-value**	**P-value**	**Estimate**	**s.e.**	**t-value**	**P-value**
Mean Model	Constant	5.1791	0..27784	18.641	<0.0001	4.9439	0.28594	17.290	<0.0001
	BMI (x2)	0.0455	0.01066	4.265	<0.0001	0.0465	0.01101	4.226	<0.0001
	Insulin (x4)	-0.0265	0.00449	-5.900	<0.0001	-0.0225	0.00494	-4.566	<0.0001
	Leptin (x6)	-0.0192	0.00336	-5.730	<0.0001	-0.0174	0.00345	-5.038	<0.0001
	Insulin *Leptin	0.0009	0.00017	5.458	<0.0001	0.0009	0.00018	4.846	<0.0001
	Resistin (x8)	0.0220	0.00348	6.327	<0.0001	0.0239	0.00345	6.923	<0.0001
Dispersion Model	Constant	0.7374	1.5228	0.484	0.6293	1.0110	1.5513	0.652	0.5158
	Age (x1)	-0.0293	0.0161	-1.826	0.0706	-0.0328	0.0156	-2.097	0.0383
	Insulin (x4)	-0.0868	0.0733	-1.184	0.2390	-0.0613	0.0720	-0.851	0.3966
	Age* Insulin	0.0051	0.0016	3.098	0.0025	0.0054	0.0015	3.488	0.0008
	HOMA-IR (x5)	-0.8286	0.2928	-2.830	0.0055	-0.9607	0.2825	-3.400	0.0009
	Glucose (x3)	0.0053	0.0144	0.371	0.7113	0.0069	0.0143	0.483	0.6300
	Leptin (x6)	-0.0997	0.0421	-2.365	0.0198	-0.1177	0.0416	-2.826	0.0056
	Glucose* Leptin	0.0007	0.0004	1.756	0.0819	0.0008	0.0004	2.091	0.0388
	Resistin (x8)	-0.0405	0.0227	-1.781	0.0777	-0.0524	0.0224	-2.332	0.0215
	Leptin*Resistin	0.0010	0.0004	2.411	0.0176	0.0013	0.0004	3.114	0.0024
		AIC=1572.816				AIC=1575			

Biomarker adiponectin analysis is given by Das and Lee [21], and for ready reference it is reproduced in Table 3. Fitted adiponectin mean & dispersion models are as follows.

Adiponectin Gamma fitted mean ($\hat{\mu}$) model (from Table 3) is

$\hat{\mu}$ = exp(6.7778 - 0.1475 BMI - 0.0617 Age + 0.0020 Age*BMI - 0.0662 Resistin + 0.0282 Leptin + 0.0018 BMI*Resistin - 0.0008 BMI*Leptin),

and Adiponectin Gamma fitted variance ($\hat{\sigma}^2$) model (from Table 3) is

$\hat{\sigma}^2$ = exp(-2.318 + 0.017Age).

 DOI: https://doi.org/10.30564/jor.v2i1.2007

Table 3. Results for mean and dispersion models for Adiponectin from Log-Normal and Gamma fit

Model	Covariate	Log-normal fit				Gamma fit			
		Estimate	**S.E.**	**t-value**	**P-value**	**Estimate**	**S.E.**	**t-value**	**P-value**
Mean	Constant	6.8667	1.0012	6.858	<0.0001	6.7778	0.9853	6.879	<0.0001
	Age (x1)	-0.0627	0.0178	-3.525	0.0006	-0.0617	0.0174	-3.550	0.0006
	BMI (x2)	-0.1512	0.0367	-4.122	<0.0001	-0.1475	0.0361	-4.087	<0.0001
	AGE*BMI	0.0020	0.0006	3.067	0.0027	0.0020	0.0006	3.214	0.0017
	Leptin (x6)	0.0217	0.0184	1.179	0.2409	0.0282	0.0180	1.566	0.1202
	Resistin (x8)	-0.0701	0.0296	-2.371	0..0195	-0.0662	0.0289	-2.293	0.0237
	BMI*Resistin	0.0020	0.0010	2.003	0.0476	0.0018	0.0010	1.886	0.0615
	BMI*Leptin	-0.0006	0.0006	-0.976	0.3312	-0.0008	0.0006	-1.372	0.1729
Dispersion	Constant	-2.325	0.6674	-3.483	0.0007	-2.318	0.6595	-3.515	0.0006
	Age (x1)	0.019	0.0114	1.690	0.0939	0.017	0.0112	1.553	0.1233
AIC		**673.8**				**673.368**			

Biomarker resistin analysis is given by Das and Lee [22], and for ready reference it is reproduced in Table 4. Fitted resistin mean & dispersion models are as follows:

Resistin Gamma fitted mean ($\hat{\mu}$) model (from Table 4) is

$\hat{\mu}$ = exp(1.6651 - 0.0306 Leptin - 0.0052 Age + 0.0888 Adiponectin + 0.5421 TYOP - 0.1087 HOMA-IR+ 0.0007 MCP-1 + 0.0015 Age*HOMA-IR - 0.0028 BMI + 0.0068 Glucose + 0.0014 BMI*Leptin - 0.0010 Glucose*Adiponectin - 0.0009 Leptin*Adiponectin),

and Resistin Gamma fitted variance ($\hat{\sigma}^2$) model (from Table 4) is

$\hat{\sigma}^2$ = exp(- 4.8464 + 0.7971 TYOP + 0.1090 BMI + 0.0129 Leptin + 0.1885 Adiponectin - 0.0083 BMI*Adiponectin).

Table 4. Results for mean & dispersion models for Resistin from Log-Normal and Gamma fit

Model	Covariates	Gamma fit				Log-normal fit			
		Estimate	**s.e.**	**t-value**	**P-value**	**estimate**	**s.e.**	**t-value**	**P-value**
Mean	Constant	1.6651	0.7909	2.105	0.0377	2.0242	0.81494	2.484	0.0146
	Age (x1)	-0.0052	0.0033	-1.547	0.1249	-0.0063	0.00345	-1.817	0.0721
	Leptin (x6)	-0.0306	0.0226	-1.352	0.1793	-0.0256	0.02334	-1.097	0.2751
	Adiponectin (x8)	0.0888	0.0553	1.607	0.1111	0.0483	0.05623	0.860	0.3917
	MCP-1 (x9)	0.0007	0.0001	4.402	<0.0001	0.0007	0.00015	4.253	<0.0001
	Patient's typ (Fx10)	0.5421	0.1084	4.999	<0.0001	0.4341	0.11120	3.904	0.0001
	HOMA-IR (x5)	-0.1087	0.0593	-1.832	0.0698	-0.1026	0.06124	-1.675	0.0969
	Age*HOMA-IR	0.0015	0.0009	1.631	0.1059	0.0016	0.00096	1.637	0.1046
	BMI (x2)	-0.0028	0.0175	-0.158	0.8747	-0.0003	0.01808	-0.015	0.9880
	Leptin*BMI	0.0014	0.0007	2.064	0.0415	0.0011	0.00072	1.529	0.1293
	Glucose (x3)	0.0068	0.0062	1.084	0.2808	0.0030	0.00650	0.456	0.6493
	Adiponectin*Glucose	-0.0010	0.0006	-1.656	0.1007	-0.0006	0.00061	-1.000	0.3196
	Leptin*Adiponectin	-0.0009	0.0005	-1.807	0.0736	-0.0006	0.00052	-1.180	0.2407
Dis-per-sion	Constant	-4.8464	1.7259	-2.808	0.0059	-4.6565	1.8505	-2.516	0.0134
	Leptin (x6)	0.0129	0.0091	1.427	0.1566	0.0124	0.0088	1.412	0.1609
	Patient's typ (Fx10)	0.7971	0.3097	2.574	0.0114	0.8184	0.3140	2.606	0.0105
	BMI (x2)	0.1090	0.0645	1.689	0.0942	0.1081	0.0690	1.567	0.1201
	Adiponectin (x7)	0.1885	0.1468	1.284	0.2020	0.1771	0.1542	1.149	0.2532
	BMI*Adiponectin	-0.0083	0.0058	-1.444	0.1518	-0.0081	0.0060	-1.342	0.1825
	AIC	**729.369**				731.2			

DOI: https://doi.org/10.30564/jor.v2i1.2007

Biomarker leptin analysis is given by Das and Lee [23], and for ready reference it is reproduced in Table 5. Fitted leptin mean & dispersion models are as follows:

Leptin Gamma fitted mean ($\hat{\mu}$) model (from Table 5) is

$\hat{\mu}$ = exp(-0.227 + 0.092 BMI + 0.006 Glucose + 0.010 Insulin + 0.025 Adiponectin + 0.016 Resistin - 0.001 MCP.1 - 0.001 Adiponectin*Resistin),

and Leptin Gamma fitted variance ($\hat{\sigma}^2$) model (from Table 5) is

$\hat{\sigma}^2$ = exp(-3.809 + 0.042 Age + 0.153 Resistin - 0.003 Age*Resistin).

Table 5. Associations of leptin with BMI, diabetes, age and breast cancer biomarkers

Response	Associated with	Types of association	P-value
Leptin mean	BMI (x2)	Directly	<0.0001
	Glucose (x3)	Directly	0.0135
	Insulin (x4)	Directly	0.0557
	Adiponectin (x7)	Directly	0.0110
	Resistin (x8)	Directly	0.0073
	MCP-1(x9)	Inversely	0.0330
	Adiponectin*Resistin	Inversely	0.0966
Leptin variance	Age (x1)	Directly	0.0034
	Resistin (x8)	Directly	0.0028
	Age*Resistin	Inversely	0.0009

3. Results

In Table 1, it is shown that mean BMI is directly associated with leptin (P<0.0001) and MCP-1 (P=0.0002), while it is inversely associated with adiponectin (P=0.0003), HOMA-IR (P<0.0001), and it is higher for healthy women (P=0.0116) than breast cancer women. In addition, variance of BMI is inversely associated with resistin (P=0.1450). On the other hand, from Table 2, mean MCP-1 is directly associated with BMI (P<0.0001). In Table 3, it is shown that mean adiponectin is inversely associated with BMI (P<0.0001), BMI*Leptin (P=0.1729), while it is directly associated with Age*BMI (P=0.0017) and BMI*Resistin (P=0.0615). From Table 4, it is noted that mean resistin is directly associated with BMI*Leptin (P=0.0415), while its variance is directly associated with BMI (P=0.0942), and it is inversely associated with BMI*Adiponectin (P=0.1518). In Table 5, it is shown that mean leptin is directly associated with BMI (P<0.0001).

4. Discussion

The summarized analyses of BMI, MCP-1, adiponection, resistin and lepin are given in Tables (1-5). From Table 1, mean BMI is directly associated with leptin (P<0.0001), or MCP-1 (P=0.0002), concluding that it increases as leptin, or MCP-1 rises. In addition, it is inversely associated with adiponectin (P=0.0003), or HOMA-IR (P<0.0001), interpreting that it increases as adiponectin, or HOMA-IR decreases. Mean BMI is inversely associated with patient types (P=0.0116), indicating that BMI is higher for healthy women than breast cancer women. Variance of BMI is partially inversely associated with resistin (P=0.1450), interpreting that BMI variance rises as resistin level decreases. It is noted that partially significant effect is treated as confounder in epidemiology.

From Table 2, it is observed that MCP-1 is directly associated with BMI (P<0.0001), indicating that it increases as BMI increases. This is also observed from the BMI model as stated above. From Table 3, it is noted that mean adiponectin is inversely associated with BMI (P<0.0001), indicating that it decreases as BMI rises. This is also observed from BMI model. Mean adiponectin is directly associated with BMI*Resistin (P=0.0615), concluding that it rises as the interaction effect BMI*Resistin increases. In addition, mean adiponectin is inversely associated with BMI*Leptin (P=0.1729), indicating that it decreases as BMI*Leptin rises. Moreover, mean adiponectin is directly associated with Age*BMI (P=0.0017), concluding that it rises as the interaction effect Age*BMI increases. This implies that over weight women at older ages have higher level of adiponectin. From Table 4, mean resistin is directly associated with the interaction effect of BMI*Leptin (P=0.0415), concluding that it rises as interaction effect of BMI*Leptin increases. Variance of resistin is directly associated with BMI (P=0.0942), interpreting that it in-

 DOI: https://doi.org/10.30564/jor.v2i1.2007

creases as BMI increases. Variance of resistin is inversely associated with BMI*Adiponectin (P=0.1518), indicating that it rises as BMI*Adiponectin decreases. From Table 5, mean leptin is directly associated with BMI (P<0.0001), indicating that it rises as BMI rises. This is also observed in BMI model. All the above summarized associations between BMI and BCBs are displayed in Table 6.

Table 6. Associations between BMI & breast cancer biomarkers

Model	Response	Associated with	Association types	P-vale
Mean	BMI (x2)	Leptin (x6)	Directly	<0.0001
		Adiponectin (x7)	Negative	0.0003
		MAC-1 (x9)	Directly	0.0002
		HOMA-IR (x5)	Inversely	<0.0001
		Patient's type (Fx10)	Inversely	0.0116
Dispersion		Resistin (x8)	Inversely	0.1450
Mean	MCP-1(x9)	BMI (x2)	Directly	<0.0001
Mean	Resistin (x8)	BMI*Leptin	Directly	0.0415
Dispersion		BMI (x2)	Directly	0.0942
		BMI* Adiponectin	Inversely	0.1518
Mean	Leptin (x6)	BMI (x2)	Directly	<0.0001
Mean	Adiponectin (x7)	BMI (x2)	Inversely	<0.0001
		Age*BMI	Directly	0.0017
		BMI*Resistin	Directly	0.0615
		BMI*Leptin	Inversely	0.1729

The present derived associations between BMI and BCBs are little compared with the previous findings as the earlier research articles have not considered all these BCBs along with BMI. In addition, the earlier articles have not considered probabilistic joint modeling to derive these associations. All these reported results herein are only based on the articles [19-23].

5. Conclusions

The report examines the associations between BMI and BCBs such as MCP-1, leptin, adiponection and resistin. These associations are reported herein considering the models of BMI and each BCB. From these models, it can be concluded that BMI and BCBs are associated in both mean and variance models. BMI increases as leptin, or MCP-1 increases, or adiponection, or resistin, or HOMA-IR decreases. Many interaction effects such as BMI*Leptin and BMI*Adiponectin are associated with resistin, while BMI*Resistin, BMI*Leptin and Age*BMI are associated with adiponectin. The report gives clear associations between BMI and BCBs which are very helpful to the researchers and medical practitioners. Medical practitioners and women should care on BMI along with breast cancer biomarkers.

Conflict of Interest

The authors confirm that this article content has no conflict of interest.

References

[1] Williams CL, Hayman LL, Daniels SR, Robinson TN, Steinberger J, Paridon S, Bazzarre T. Cardiovascular health in childhood: A statement for health professionals from the Committee on Atherosclerosis, Hypertension, and Obesity in the Young (AHOY) of the Council on Cardiovascular Disease in the Young, American Heart Association. Circulation, 2002, 106(1): 143-160.

[2] US Dept Health and Human Services. The Surgeon General's Call to Action to Prevent and Decrease Overweight and Obesity. Rockville, MD: US Department of Health and Human Services, Public Health Service, Office of the Surgeon General, 2001.

[3] National Institutes of Health. Clinical guidelines on the identification, evaluation, and treatment of overweight and obesity in adults - the evidence report. Obes Res., 1998. 6 (suppl 2): 51-209S.

[4] Gunter MJ, Xie X, Xue X, Kabat GC et al. Breast Cancer Risk in Metabolically Healthy but Overweight Postmenopausal Women. Cancer Res. 2015, 75(2): 270-274.

[5] Key TJ, Appleby PN, Reeves GK, Roddam A, Dorgan JF, Longcope C, et al. Body mass index, serum sex hormones, and breast cancer risk in postmenopausal women. J Natl Cancer Inst., 2003, 95(16): 1218-1226.

[6] International Agency for Research on Cancer, World Health Organization. Weight control and physical activity. In: Vainio H, Bianchini F, eds. International Agency for Research on Cancer handbooks of cancer prevention, Lyon, France: IARC Press, 2002, 6.

[7] Calle EE, Rodriguez C, Walker-Thurmond K, Thun MJ. Overweight, obesity, and mortality from cancer in a prospectively studied cohort of U.S. adults. N Engl J Med., 2003, 348: 1625-1638.

[8] Van Den Brandt PA, Spiegelman D, Yaun SS et al. Pooled analysis of prospective cohort studies on height, weight, and breastcancer risk. Am J Epidemiol., 2000, 152: 514-27.

[9] Morimoto LM,White E, Chen Z et al. Obesity, body size, and risk of postmenopausal breast cancer: The

DOI: https://doi.org/10.30564/jor.v2i1.2007

Women's Health Initiative (United States). Cancer Causes Control, 2002, 13: 741-51.

[10] Lahmann PH, Hoffmann K, Allen N et al. Body size and breast cancer risk: findings from the European Prospective Investigation into Cancer and nutrition (EPIC). Int J Cancer, 2004, 111: 762-71.

[11] Renehan AG, Tyson M, Egger M, Heller RF, Zwahlen M. Bodymass index and incidence of cancer: a systematic review and meta-analysis of prospective observational studies. Lancet, 2008; 371:569-78.

[12] Cecchini RS, Costantino JP, Cauley JA et al. Body mass index and the risk for developing invasive breast cancer among high risk women in Nsabp P-1 and Star Breast Cancer Prevention

Trials. Cancer Prev Res (Phila), 2012,5: 583-92.

[13] Macis D, Guerrieri-Gonzaga A, Gandini S. Circulating adiponectin and breast cancer risk: a systematic review and meta-analysis. International Journal of Epidemiology, 2014: 1226-1236.

[14] Dumitrescu RG, Cotarla I. Understanding breast cancer risk - where do we stand in 2005? J Cell Mol Med., 2005, 9: 208-221.

[15] Crisóstomo J, Matafome P, Santos-Silva D, Gomes AL, Gomes M, et al. Hyperresistinemia and metabolic dysregulation: a risky crosstalk in obese breast cancer. Endocrine, 2016, 53(2): 433-442.

[16] Patrício M, Pereira J, Crisóstomo J, Matafome P, Gomes M, Seiça R, Caramelo F. Using Resistin, glucose, age and BMI to predict the presence of breast cancer. BMC Cancer, 2018, 18(1): 18-29.

[17] Paz-Filho G, Lim EL, Wong ML, Licinio J. Associations between adipokines and obesity-related cancer. Front Biosci., 2011, 16: 1634-1650.

[18] Steppan CM, Bailey ST, Bhat S, Brown EJ, Banerjee RR, et al. Thehormoneresistin links obesity to diabetes. Nature, 2001, 409: 307-312.

[19] Das RN, Lee Y, Mukherjee S, Oh S. Relationship of body mass index with diabetes & breast cancer biomarkers. J Diabetes and Management, 2019,. 9(1): 163-168.

[20] Kim J, Das RN, Lee Y, Sahoo RK. Association of monocyte chemoattractant protein-1 with age, glucose, BMI, insulin and other breast cancer biomarkers. Oncology and Radiotherapy, 2019, 13(1): 005-009.

[21] Das RN, Lee Y. Association of Serum Adiponectin with Age, BMI and Other Breast Cancer Biomarkers. J Blood Lymph, 2018, 8(4): 233.

[22] Das RN, Lee Y. Association of resistin with BMI, age diabetes and breastcancer biomarkers. Journal of Oncology Research and Treatment, 2019, 4(1): 135.

[23] Das RN, Lee Y. Relationship of leptin with glucose, BMI, age, insulin and breast cancer biomarkers. Arch Gen Intern Med., 2019, 3(1): 01-03.

[24] Lee Y, Nelder JA, Pawitan Y. Generalized Linear Models with Random Effects (Unified Analysis via H-likelihood). Second Edition, London: Chapman & Hall, 2017.

[25] Das RN, Lee Y. Log-normal versus gamma models for analyzing data from quality-improvement experiments. Quality Engineering, 2009, 21(1): 79-87.

[26] Lesperance ML, Park S. GLMs for the analysis of robust designsvwith dynamic characteristics. Journal Quality Technology, 2003, 35: 253-263.

 DOI: https://doi.org/10.30564/jor.v2i1.2007

BILINGUAL PUBLISHING CO.
Pioneer of Global Academics Since 1984

Journal of Oncology Research
https://ojs.bilpublishing.com/index.php/jor

ARTICLE

Application of AI Technology in Tumor medical Imaging

Tong Li[1*] Yi Xie[2] Jingxiong Chen[1]

1. Beijing Gaobo Hospital Management Co., Ltd., Beijing, 100000, China
2. Beijing Anxun Dasheng Technology Co., Ltd., Beijing, 100000, China

ARTICLE INFO

Article history
Received: 22 June 2020
Accepted: 22 June 2020
Published: 30 June 2020

Keywords:
Artificial intelligence
Algorithms
Deep learning
Oncology
Medical imaging

ABSTRACT

Artificial intelligence AI has many algorithms, , there are many applications in central nervous system tumors, lung cancer, breast cancer, prostate cancer, orthopaedic tumors, etc., with the norms and support of national policies,AI technology in tumor medical imaging will be ushed broadly.

1. Introduction

The term "artificial intelligence" was first introduced and adopted at the Dartmouth College Symposium in 1956, and since the beginning of the 21st century,the research and application of AI in medical imaging has developed rapidly, especially in tumor imaging, and there have been more clinical research and applications in tumor detection, qualitative diagnosis, automatic structured reporting, tumor extraction, and tumor radiation target organ sketching.

2. The Classic AI Algorithm and Its Application in Medical Imaging

The current classical AI algorithm can be summarized as a collection theory classification, based on probability statistical classification, graph-based classification, spatial geometric classification, based on cross-disciplinary classification, and so on, each classification contains some commonly used algorithms, such as the artificial intelligence algorithm based on probability statistics has simple Bayes, logic regression, maximum entropy,etc.The deep learning algorithm which simulates human neural network is one of the algorithms belonging to the interdisciplinary classification.

3. Application of AI Technology in Medical Imaging

According to statistics,more than 90% of the information stored in hospitals comes from medical imaging equipment,AI in medical imaging equipment can make low-dose CT, PET images by reconstructing high-dose images, reduce radiation risk; AI has also made some substantial

**Corresponding Author:*
Tong Li,
Beijing Gaobo Hospital Management Co., Ltd., Beijing, 100000, China;
Email: 2562275375@qq.com

DOI: https://doi.org/10.30564/jor.v2i1.2026

developments in the diagnosis of ultrasound imaging and the analysis of pathological slicing. In terms of intelligent services, Medical Imaging AI provides intelligent services ranging from assisted detection, assisted diagnostics, accurate diagnosis, quantitative follow-up to precision therapy. Image classification, target detection, object segmentation and image generation are key issues in AI image processing, which are particularly important in medical imaging analysis and processing [1]. Deep learning is a very wide range of algorithms, common types include regional convolutional neural network algorithms, spatial pyramid pooling algorithms, fast R-CNN algorithms, Faster R-CNN algorithms, YOLO algorithms, etc. In addition, more and more target detection algorithms are now abandoning the design of anchorbox. One of the most innovative target detection algorithms is called detr. This algorithm extracts features from the input picture, adds position coding, puts it into the transformer, and directly gets the target location, size, and category. This novel design completely abandons post-processing, reduces the need for calculation of target detection, and improves the efficiency of target detection [2].

4. The Application of AI Technology in Tumor Imaging

4.1 Application of Artificial Intelligence in Central Nervous System Tumors

The purpose of brain tumor segmentation is to identify the location of the tumor and the area where the tumor is immersed outward, i.e. to identify tumor tissue, necrotic tissue, and surrounding edema. Soltaninejad et al. [3], using machine learning algorithms based on 3D Super voxel, analyzed MR images from 2 clinical databases (11 samples and 30 cases, respectively) with Dice coefficient of 0.84, 0.89,which have high accuracy. On the basis of identifying and dividing brain tumors, artificial intelligence algorithms can also be used to grade gliomas, identify glioma recurrence and post-treatment necrosis, prognosis prediction of gliomas, and predict the prognosis of gliomas.

4.2 Applications of Human Intelligence in Lung Cancer

Artificial intelligence has shown good clinical application value in lung cancer detection and staging. Masood et al.used deep learning algorithm to analyze chest CT images from multiple databases, and the average accuracy of diagnosis reached 84.58%, and the accuracy of lung cancer t1-T4 staging reached 77.89% ~ 90.14%. Sun et al. conducted a comparative study on deep learning algorithm and traditional shallow learning algorithm. The data came from Lung Image Database Consortium (LIDC), which contained 13,668 chest CT images. The results showed that the AUC of deep learning was 0.899±0.018 and that of shallow learning was 0.848±0.026 [4]. Artificial intelligence identification of pulmonary nodules is also a major research direction for domestic companies.

4.3 Applications of Artificial Intelligence in Breast Cancer

In 2016,Quellec et al. proposed a new computer-aided detection and diagnosis system for mammography, which relies on the MIL(a weak supervised learning method) paradigm and uses only whole-image level labels. They first divide the breast adaptively into multiple regions, then extract and combine features of detected lesions from each region to classify mammograms as normal or abnormal. Becker et al. applied deep learning algorithm to classify 632 patients (550 benign and 82 malignant). The total time of computer classification of benign and malignant was 3.7s and the AUC could reach 0.84.The three doctors with high to low experience spent 28 minutes, 22 minutes and 25 minutes respectively, with an AUC of 0.79 ~ 0.88, indicating that artificial intelligence can achieve similar accuracy in the classification of benign and malignant breast cancer as imaging doctors, and can significantly improve work efficiency.

4.4 Application Sofa in Prostate Cancer

In western countries Prostate cancer is the first incidence of malignant tumors in male, in recent years, the incidence of China has also shown a clear upward trend. Wang et al. compared the diagnostic accuracy of deep learning algorithms and non-deep learning algorithms in prostate cancer and benign hyperplasia based on MR images, the AUC of Deep Learning AUC was 0.83 and the AUC of non-deep learning algorithm was only 0.70, that means it is better to use depth study to identify the performance.

4.5 Application of Artificial Intelligence in Bone Tumors

The quality of life of patients with spinal metastases is significantly reduced, so early detection has great significance.Wang et al.used deep learning algorithm to analyze the sagittal MR images of the spine of 26 patients with spinal metastasis. After combining the analysis results of the twin neuron network, the diagnostic sensitivity reached 90%.

In addition to the above-mentioned tumors, AI has also

 DOI: https://doi.org/10.30564/jor.v2i1.2026

been used in other tumors such as liver tumors.

5. Industrial Status of Medical Imaging Artificial Intelligence in China

In July 2017, China released the Development Plan for The Next Generation of Artificial Intelligence, which proposes the development of intelligent disease prediction, intelligent diagnosis, intelligent treatment mode and intelligent medical system.The establishment of medical imaging AI model often needs a large amount of data support, at this stage, each research team is prone to form data silos, data labeling consistency is low, gold standard is missing, and quality control, data security and privacy protection are also problems, there are significant differences in the understanding and implementation ability of various participants in medical imaging AI. From ethical point of view, the current research on medical imaging AI is still insufficient to pay attention to the questions of the patient's right to know, privacy protection and other medical ethics issues, data security issues and the safety of patients' treatment [5].

Among the physicians and researchers in China, young and middle-aged physicians, senior doctors and radiologists are generally concerned about AI technology, and the researchers involved in AI research are mostly young students, preferring to be younger, which brings broad prospects for the development of the AI industry. In addition [6], China's hospitals need to improve the current system of talent introduction, attract high-end talent in China's medical imaging in the field of artificial intelligence innovation and development, is conducive to China's medical imaging AI industry towards the direction of standardization and normalization.

References

[1] Dong Meng jie,et al. Artificial intelligence in medical imaging. Int J Radiat Med Nucl Med. January 2020, 44(1).

[2] Nicolas Carion,et al. End to End Object Detection with Transformers.ar Xiv: 2005.12872v1 [cs.CV] 26 May 2020.

[3] Soltaninejad M, Yang G, Lambrou T, et al. Supervised learning based multimodal MRI brain tumour segmentation using texture features from supervoxels. Comput Methods Programs Biomed, 2018, 157: 69-84.

[4] W Sun, B Zheng, W Qian. Automatic feature learning using multichannel ROI based on deep structured algorithms for computerized lung cancer diagnosis. Comput Biol Med, 2017, 89: 530-539.

[5] Qiang Xu, et al. Current and challenge in clinical transformation of the new generation of artificial intelligence in medical imaging. Chin J Radiol, November 2019, 53(11).

[6] Zhang Huimao, et al. The report of status and needs in medical imaging artificial intelligence industry. Chin J Radiol, 2019, 53(6).

DOI: https://doi.org/10.30564/jor.v2i1.2026

BILINGUAL PUBLISHING CO.
Pioneer of Global Academics Since 1984

Journal of Oncology Research
https://ojs.bilpublishing.com/index.php/jor

REVIEW

Progress in Diagnosis and Treatment of Basal Cell Carcinoma

Yan Liu Mengxian Ren* Youfei Zhao Dong Liu Fei Zhou

Anhui Taihe County People's Hospital, Taihe, Anhui, 236600, China

ARTICLE INFO

Article history
Received: 22 June 2020
Accepted: 22 June 2020
Published: 30 June 2020

Keywords:
Basal cell carcinoma
Diagnosis and treatment

ABSTRACT

Basal cell carcinoma is a common skin carcinogenesis that occurs in the epidermis and the basal layer of the skin.in general, basal cell carcinoma grows slowly, rarely metastasizes, but is locally invasive and destructive. The diagnosis is based on clinical manifestations, but the clinicopathological manifestations are different, and sometimes it is difficult to differentiate from pigmented nevus, malignant melanoma, etc. Therefore, skin biopsy is essential for the diagnosis and assessment of the risk of recurrence.There are many ways to treat basal cell carcinoma. This article reviews the diagnosis and treatment.

1. Introduction

Basal cell carcinoma is a common skin cancer, often occurs on sun-exposed skin, common parts such as face, neck, hand, etc. Most basal cell carcinoma grow slowly, they are locally invasive and can destroy surrounding tissues [1]. The main causes of the disease are ultraviolet radiation, prolonged exposure to arsenic-contaminated water, food and drugs, or increased risk factors for human immunodeficiency virus infection and immunosuppression [2].

2. Diagnosis

The diagnosis of basal cell carcinoma depends on clinical manifestation, dermoscopy and histology. Dermoscopy will improve the diagnostic accuracy of skin lesions [3]. However, skin biopsy is essential for the diagnosis and assessment of the risk of recurrence. Histopathologically, basal cell carcinoma is usually composed of uniformly proliferating basal cell-like cells with dense nuclei, relatively few cytoplasm and unclear boundaries [4]. In histopathology, nodular lesions are formed by the proliferation of large basal cells, forming huge tumor nests, surrounded by palisades, with irregular central arrangement [5]. Histopathologically, a sclerosing collagen stroma encapsulates a narrow cell chain and a small island of tumor cells. Fibroepithelial type usually occurs in the lower back, presenting as skin color or erythema soft papules or pedicle papular nodular lesions similar to fibroma or papilloma [6].

3. Treatment

Surgical resection is the standard treatment for basal cell carcinoma. The study of surgical margin may realize complete resection of tumor at different anatomical locations. It is reported that the 5-year cure rate of 4-5 mm surgical margin is 9.95% [7]. Electro-drying and curettage is the removal of the surface of the tumor with a blade or a curettage device, and the burning of the remaining substrate with an electroacupuncture to control bleeding and destroy residual tumor cells. This method is simple but can not fully demonstrate that the tumor has been removed

**Corresponding Author:*
Mengxian Ren,
Anhui Taihe County People's Hospital, Taihe, Anhui, 236600, China;
Email: 1328108798@qq.com

 DOI: https://doi.org/10.30564/jor.v2i1.2038

and is more suitable for basal cell carcinoma located in low-risk areas without invasive histopathological features [8]. cryosurgery liquid nitrogen acts directly on tumors, can form extracellular and intracellular ice crystals, destroy cell phospholipid membranes, and destroy peripheral tumor-associated blood vessels for therapeutic purposes, but can not be histologically confirmed. cryosurgery can not be used as a first-line treatment for basal cell carcinoma, especially for tumors with a high risk of recurrence.topical imiquimod cream is an immune response regulator that induces cytokine production, stimulates cellular immunity, and promotes apoptosis by bypassing anti-apoptotic mechanisms of tumor cells [9]. The curative effect is not as good as the local operation, the systemic side effect is many, usually uses in the low-risk position superficial basal cell carcinoma treatment. Local fluorouracil by inhibiting thymidine synthase interference DNA synthesis, local application of 5% FU cream has been proved to be generally effective, local fluorouracil is usually used only for superficial basal cell carcinoma in non-critical anatomical area, while for nodular or invasive basal cell carcinoma, it is generally forbidden [10]. light energy therapy, because reactive oxygen species produced by photosensitizers selectively absorb light induces cytotoxicity in tumor cells and local inflammatory responses that may lead to tumor destruction, complete tumor resection depends on the concentration of photosensitizers in tumor cells and the ability of light focusing in related regions.the effect of radiotherapy is positive, but recurrent basal cell carcinoma after radiotherapy may exhibit greater aggressiveness, including second recurrence and distant metastasis. in addition, the evidence of long-term efficacy of radiotherapy is limited. common side effects include chronic radiation dermatitis, permanent alopecia, dermal and subcutaneous fibrosis, necrosis, and secondary cutaneous malignancies. therefore, radiotherapy is generally applicable to patients not suitable for surgery, especially in high-risk areas [11].

4. Conclusion

To sum up, preclinical and pathological assessment of recurrence risk is necessary to select the best treatment strategy. According to the location of the tumor, the pathological subtype, the patient's condition, the beauty effect and the cost of treatment, different treatment methods can be used.

References

[1] Lo J, Snow S, Reizner G. Metastatic basal cell carcinoma: a report of twelve cases with a review of the literature. J Am Acad Dermatol., 1991, 24: 715-9.

[2] Karagas MR, Tosteson TD, Blum J, Morris JS, Baron JA, Klaue B. Design of an epidemiologic study of drinking water arsenic exposure and skin and bladder cancer risk in a U.S. population. Environ Health Perspect, 1998, 106(Suppl. 4): 1047-50.

[3] Altamura D, Menzies SW, Argenziano G, Zalaudek I, Soyer HP, Sera F, et al.Dermatoscopy of basal cell carcinoma: morphologic variability of global and local features and accuracy of diagnosis.J Am Acad Dermatol., 2010, 62: 67-75.

[4] Patterson JW. Weedon's skin pathology. 4th ed. London: Churchill-Livingstone, 2016: 806-11.

[5] Sexton M, Jones DB, Maloney ME. Histologic pattern analysis of basal cell carcinoma. Study of a series of 1039consecutive neoplasms. J Am Acad Dermatol., 1990, 23: 1118-26.

[6] Rosai J. Rosai, Ackerman's surgical pathology. 9th ed. Edinburgh: Mosby, 2004: 136-9.

[7] Scrivener Y, Grosshans E, Cribier B. Variations of basal cell carcinomas according to gender, age, location and histopathological subtype. Br J Dermatol., 2002, 147: 41-7.

[8] Silverman MK, Kopf AW, Bart RS, Grin CM, Levenstein MS. Recurrence rates of treated basal cell carcinomas. Part 3: surgical excision. J Dermatol Surg Oncol., 1992, 18: 471-6.

[9] Blixt E, Nelsen D, Stratman E. Recurrence rates of aggressive histologic types of basal cell carcinoma after treatment with electrodesiccation and curettage alone. Dermatol Surg., 2013, 39: 719-25.

[10] Geisse J, Caro I, Lindholm J, Golitz L, Stampone P, Owens M. Imiquimod 5% cream for the treatment of superficial basal cell carcinoma: results from two phase III, randomized, vehicle-controlled studies. J Am Acad Dermatol., 2004, 50: 722-33.

[11] Foley P. Clinical efficacy of methyl aminolevulinate (Metvix) photodynamic therapy. J Dermatolog Treaty, 2003, 14(Suppl 3): 15-22.

DOI: https://doi.org/10.30564/jor.v2i1.2038

BILINGUAL PUBLISHING CO.
Pioneer of Global Academics Since 1984

Journal of Oncology Research
https://ojs.bilpublishing.com/index.php/jor

REVIEW

The Clinical Application Value of Susceptibility Weighted Imaging in the Central Nervous System

Haichao Fu*

Inner Mongolia Medical University, Hohhot, Inner Mongolia, 010059, China

ARTICLE INFO

Article history
Received: 20 July 2020
Accepted: 22 July 2020
Published: 18 August 2020

Keywords:
Susceptibility weighted imaging
Central nervous system diseases
Magnetic resonance imaging

ABSTRACT

Susceptibility weighted imaging (SWI) is a relatively new magnetic resonance imaging (MRI) technique that uses the difference in tissue magnetic susceptibility to image, and has unique value compared to traditional magnetic resonance imaging. This article summarizes its application in the central nervous system and provides a reference for imaging diagnosis and clinical treatment.

1. Introduction

Susceptibility weighted imaging (SWI) is a non-invasive magnetic resonance imaging technique that takes advantage of the difference in magnetic properties of different tissues. It is based on a new long echo time, complete flow compensation, and three-dimensional gradient imaging sequence.Compared with the traditional T2* weighted sequence, it has the characteristics of three-dimensionality, high resolution, and high signal-to-noise ratio.The original SWI image is the Magnitude image and the Phase image obtained by scanning the T2* weighted echo sequence. The two can be analyzed separately or processed for image fusion. The Magnitude image contains most of the tissue contrast information, and the Phase image reflects the tissue contrast from the perspective of susceptibility, especially the tissues with large differences in magnetic susceptibility. These two images are obtained at the same time during the scanning process, always appearing in pairs, and the anatomical position corresponding to each pair of images is exactly the same.

SWI is very sensitive to display venous structure, blood metabolites (such as deoxyhemoglobin), iron deposition, calcification, etc. Even without the use of contrast agents, it can clearly show the vascular system and hemorrhagic components, so it is used in cerebrovascular diseases, brain Tumors, brain trauma, neurodegenerative diseases and other central nervous system diseases have high clinical application prospects and value. SWI has now become a key magnetic resonance imaging sequence for the diagnosis of central nervous system diseases, and is an effective supplement to traditional spin echo magnetic resonance imaging sequences. In recent years, quantitative magnetic susceptibility mapping(QSM) that can quantitatively analyze tissue magnetic susceptibility have emerged based on SWI further makes up for the shortcomings of SWI [1]. This article will

**Corresponding Author:*
Haichao Fu,
Inner Mongolia Medical University, Hohhot, Inner Mongolia, 010059, China;
Email: 1149221898@qq.com

 DOI: https://doi.org/10.30564/jor.v2i1.2192

analyze the clinical application value of SWI in the central nervous system from the following points.

2. Cerebrovascular Disease

Biological tissue generates a specific induced magnetic field under the action of an external magnetic field, which depends on the strength of the external magnetic field and the magnetic sensitivity of tissue molecules. Magnetic susceptibility can be measured by the magnetic susceptibility. The degree of magnetization of the reaction material under the action of an external magnetic field is a variable reflecting the organization. The oxygenation and deoxygenation conversion of hemoglobin is the basis of blood oxygen level-dependent imaging. Oxyhemoglobin is diamagnetic, deoxyhemoglobin has 4 unpaired electrons that are paramagnetic, and hemoglobin is a strong paramagnetic substance but has weak magnetic sensitivity, hemosiderin is a paramagnetic substance, deoxyhemoglobin and hemosiderin have strong magnetic sensitivity. Non-heme iron (often in the form of ferritin) is a paramagnetic substance and has a strong magnetic sensitivity effect. The magnetic sensitivity effect of calcification is weaker than that of iron. It is usually diamagnetic. On the SWI corrected phase image, the right-hand magnetic resonance imaging system (United States GE, Philips) showed calcification as a high signal, while the signal in the left-hand MRI system (Siemens, Germany) was opposite. Studies have shown that SWI also has significant advantages in the detection of calcium, and it is the only imaging method that can distinguish bleeding and calcification at the same time [2].

Cerebral microbleeds (CMBs), as a marker of small blood vessel diseases in the brain, is more sensitive than other sequences in displaying microbleeds in the brain, and it is currently the best imaging method for the diagnosis of CMBs[3,4].Studies have shown that the prevalence of CMBs in healthy people is 5%, the prevalence of ischemic stroke patients is 22.9% -43.6%, and the incidence of hemorrhagic stroke patients and mixed stroke patients are respectively As high as 51.8% -82.5% and 41.2% -70.2% [5].Cerebral microhemorrhage is mainly caused by the deposition of hemosiderin and mononuclear macrophages that have swallowed hemosiderin, which leads to local arteriole hyaloid degeneration and amyloid deposition [6]. Therefore, CMBs appear on SWI as clear edges and uniform properties. The diameter is between 2-5mm (the highest is no more than 10mm), and the shape is a round or oval low signal or lack of signal focus, without edema around it [7].

3. Brain Tumors

Conventional MRI examination sequence is difficult for the preoperative grading diagnosis of brain tumors, and the use of SWI to evaluate the angiogenesis and intratumor hemorrhage within the tumor is an effective supplement to the conventional MRI examination.In addition to distinguishing bleeding and calcification in brain tumors, SWI can clearly show the neovascular structure in the tumor and the blood oxygen status inside the tumor, which is of great significance for the staging and grading of the tumor [8]. At the same time, SWI is proposed to be used To evaluate the effects and differences of different anti-vascular gene drugs, as well as the diagnosis of curative effects after radiotherapy and chemotherapy, the progression of tumors can be studied longitudinally.Studies have shown that high-grade tumors generally have rapid growth and a large number of new pathological blood vessels and are prone to bleeding and necrosis; on the contrary, low-grade tumors often appear calcification due to slow growth and malnutrition [9].Grading and scoring using intratumoral susceptibility signalintensity (ITSS) is considered to be related to its pathological grading and is an important basis for distinguishing benign and malignant tumors [10].

4. Brain Injury

Diffuse axonal injuries (DAI) is the most common type of brain trauma. It is caused by the shear force formed during the acceleration or deceleration of the head. Its common occurrence areas include the junction of the gray matter of the brain, The pressure part of the corpus callosum, the basal segment area and the dorsal side of the brain stem, etc., can detect punctate microhemorrhages in the deep white matter that cannot be displayed by CT or conventional MRI sequences.A study specifically for patients with mild traumatic brain injury compared the results of CT and SWI. The conclusion showed that the detection rate of SWI was as high as 97.83%, especially for brain contusion and laceration [11]. The detection rate was significantly higher than that of CT.It is more sensitive to traumatic brain injury and can accurately assess the patient's prognosis.

5. Central Nervous System Degenerative Disease

Central nervous system degenerative disease is a chronic progressive neurodegenerative disease. Studies have shown that the increase of iron in the brain is related to the increase of age [12]. The abnormal iron metabolism is a significant feature of central nervous system degenerative diseases, including Parkinson's disease (PD), Alzheimer's disease (AD) and multiple sclerosis (MS), etc. SWI can accurately analyze the distribution range and amount of iron

DOI: https://doi.org/10.30564/jor.v2i1.2192

deposits in the brain. The detection provides a safe, simple and non-invasive inspection method, and is clearer than conventional sequences. The etiology of PD is due to abnormal iron metabolism resulting in increased iron deposits in the substantia nigra and striatum, leading to progressive loss of dopaminergic neurons, resulting in increased muscle tone, resting tremor, retardation of movement, postural balance disorders, and a series of clinical symptom. Studies have shown that [13] possible signal changes related to iron deposition on SWI can accurately distinguish PD from various other forms of Parkinson's disease. At the same time, the FA value of the substantia nigra and the size of the substantia nigra compact zone are helpful for the early diagnosis of PD. By measuring the signal intensity of related brain nuclei and calculating the phase value, it can evaluate brain iron deposition, which is the treatment and treatment of PD patients. Provide help for the subsequent effect evaluation. For AD, studies have shown that [14] the vast majority of AD patients are transformed from mild cognitive impairment (MCI). SWI can not only intervene in the conversion process from MCI to AD, but also monitor iron deposition during the conversion process. In order to guide clinical diagnosis and treatment in the early stage of dementia.

SWI is a relatively new imaging method, which has great development prospects in the diagnosis and treatment of central nervous system diseases. However, SWI still has some shortcomings. For example, SWI has a long scanning time and requires a long inspection site. The time limit is temporarily not suitable for tissues and organs with greater mobility. At the same time, parts with extremely large differences in magnetic susceptibility (air-tissue plane) such as the level of the skull base and sinuses will cause heavier artifacts and have "magnification effects", which affect the observation and evaluation of lesions. These challenges require further research and improvement by technicians and scientific researchers. It is believed that with the development and progress of science and technology, SWI's diagnosis of diseases will become deeper and deeper, and it will no longer be limited to the central nervous system.

References

[1] Xin Cao, Hao Shi. The latest clinical application and development of susceptibility weighted imaging[J]. Chinese Journal of Neurology, 2018, 51(7): 550-555.

[2] Di leva A, Lam T, Alcaide-Leon P, et al. Magnetic resonance susceptibility wei-ghted imaging in neurosurgery:current applications and future perspectives[J]. J Neurosurg, 2015, 123(6): 1463-1475.

[3] Haller S,Vernooij M,Kuijer J P A, et al. Cerebral Microbleedings:Imaging and Clinical Significance[J]. Radiology, 2018, 287(1):1 1-28.

[4] Bin Ye, Liling Long. Application of susceptibility weighted imaging in cerebral infarction and related diseases[J]. Guangxi Medical Journal, 2018, 40(11): 1246-1248.

[5] Lee J, Sohn EH, Oh E, et al. Characteristics of Cerebral Microbleeds[J].Dement Neurocogn Disord, 2018, 17(3): 73-82.

[6] Fazekas F,Kleinert R,Roob G,et al.Histopathologic analysis of foci of signalloss on gradient-echo T2*-weighted MR images in patients with spontaneous intracerebral hemorrhage: evidence of microangiopathy-related microbleeds[J]. AJNR.American journal of neuroradiology, 1999, 20(4): 637-642.

[7] Ge L, Ouyang X, Ban C, et al. Cerebral microbleeds in patients with ischemic ce-rebrovascular dis-ease taking aspirin or clopidogrel[J]. Medicine, 2019, 98(9): e14685.

[8] Van CS, De KF, Sima DM, et al. Integrating diffusion kurtosis imaging,dynamic s-usceptibility-weighted contrast-enhanced MRI, and short echo time chemical shiftimaging for grading gliomas[J]. Neuro-oncology, 2014, 16(7): 1010-1021.

[9] Yuejie Chen, Yanling Huang, Yongfeng Wang, et al. The value of susceptibility weighted imaging in evaluating the grading of glioma[J]. Chinese medical imaging technology, 2010, 26(2): 247-249.

[10] J. Furtner, V. Schöpf, M. Preusser, et al. Non-invasive assessment of intratumoral vascularity using arterial spin labeling: A comparison to susceptibility-weight-ed imaging for the differentiation of primary cerebral lymphoma and glioblasto-ma[J]. European Journal of Radiology, 2014, 83(5): 806-810.

[11] Haiyong Zeng, Cuiping Zhou, Guohua He, et al. Diagnosis and application evaluation of susceptibility weighted imaging in mild traumatic brain injury[J]. Chinese Practical Medicine, 2018, 13(14): 23-24.

[12] Buijs M, Doan NT, van Rooden S, et al. In vivo assessment of iron content of the cerebral cortex in healthy aging using 7-Tesla T2*-weighted phase imaging[J]. Neurobiology of Aging, 2017, 53(5): 20-26.

[13] Haller S, Badoud S, Nguyen D, Barnaure I, Montandon M-L, Lovblad K-O, Burkhard P R. Differentiation between Parkinson disease and other forms of Parkinsonism using support vector machine analysis of susceptibility-weighted imaging (SWI): initial results[J]. European radiology, 2013, 23(1): 12-19.

[14] Qingling Huang, Wen Liu, Chaoyong Xiao, et al. Diagnosis of mild cognitive impairment and Alzheimer's disease with 3T SWI small hypointense lesions[J]. Journal of medical imaging, 2015, 25(3): 381-385.

 DOI: https://doi.org/10.30564/jor.v2i1.2192

Author Guidelines

This document provides some guidelines to authors for submission in order to work towards a seamless submission process. While complete adherence to the following guidelines is not enforced, authors should note that following through with the guidelines will be helpful in expediting the copyediting and proofreading processes, and allow for improved readability during the review process.

Ⅰ. Format

- Program: Microsoft Word (preferred)
- Font: Times New Roman
- Size: 12
- Style: Normal
- Paragraph: Justified
- Required Documents

Ⅱ. Cover Letter

All articles should include a cover letter as a separate document.

The cover letter should include:

- Names and affiliation of author(s)

The corresponding author should be identified.

Eg. Department, University, Province/City/State, Postal Code, Country

- A brief description of the novelty and importance of the findings detailed in the paper

Declaration

v Conflict of Interest

Examples of conflicts of interest include (but are not limited to):

- Research grants
- Honoria
- Employment or consultation
- Project sponsors
- Author’s position on advisory boards or board of directors/management relationships
- Multiple affiliation
- Other financial relationships/support
- Informed Consent

This section confirms that written consent was obtained from all participants prior to the study.

- Ethical Approval

Eg. The paper received the ethical approval of XXX Ethics Committee.

- Trial Registration

Eg. Name of Trial Registry: Trial Registration Number

- Contributorship

The role(s) that each author undertook should be reflected in this section. This section affirms that each credited author has had a significant contribution to the article.

1. Main Manuscript
2. Reference List
3. Supplementary Data/Information

Supplementary figures, small tables, text etc.

As supplementary data/information is not copyedited/proofread, kindly ensure that the section is free from errors, and is presented clearly.

Ⅲ. Abstract

A general introduction to the research topic of the paper should be provided, along with a brief summary of its main results and implications. Kindly ensure the abstract is self-contained and remains readable to a wider audience. The abstract should also be kept to a maximum of 200 words.

Authors should also include 5-8 keywords after the abstract, separated by a semi-colon, avoiding the words already used in the title of the article.

Abstract and keywords should be reflected as font size 14.

Ⅳ. Title

The title should not exceed 50 words. Authors are encouraged to keep their titles succinct and relevant.

Titles should be reflected as font size 26, and in bold type.

Ⅳ. Section Headings

Section headings, sub-headings, and sub-subheadings should be differentiated by font size.

Section Headings: Font size 22, bold type

Sub-Headings: Font size 16, bold type

Sub-Subheadings: Font size 14, bold type

Main Manuscript Outline

Ⅴ. Introduction

The introduction should highlight the significance of the research conducted, in particular, in relation to current state of research in the field. A clear research objective should be conveyed within a single sentence.

Ⅵ. Methodology/Methods

In this section, the methods used to obtain the results in the paper should be clearly elucidated. This allows readers to be able to replicate the study in the future. Authors should ensure that any references made to other research or experiments should be clearly cited.

Ⅶ. Results

In this section, the results of experiments conducted should be detailed. The results should not be discussed at length in

this section. Alternatively, Results and Discussion can also be combined to a single section.

Ⅷ. Discussion

In this section, the results of the experiments conducted can be discussed in detail. Authors should discuss the direct and indirect implications of their findings, and also discuss if the results obtain reflect the current state of research in the field. Applications for the research should be discussed in this section. Suggestions for future research can also be discussed in this section.

Ⅸ. Conclusion

This section offers closure for the paper. An effective conclusion will need to sum up the principal findings of the papers, and its implications for further research.

Ⅹ. References

References should be included as a separate page from the main manuscript. For parts of the manuscript that have referenced a particular source, a superscript (ie. [x]) should be included next to the referenced text.

[x] refers to the allocated number of the source under the Reference List (eg. [1], [2], [3])

In the References section, the corresponding source should be referenced as:

[x] Author(s). Article Title [Publication Type]. Journal Name, Vol. No., Issue No.: Page numbers. (DOI number)

Ⅺ. Glossary of Publication Type

J = Journal/Magazine

M = Monograph/Book

C = (Article) Collection

D = Dissertation/Thesis

P = Patent

S = Standards

N = Newspapers

R = Reports

Kindly note that the order of appearance of the referenced source should follow its order of appearance in the main manuscript.

Graphs, Figures, Tables, and Equations

Graphs, figures and tables should be labelled closely below it and aligned to the center. Each data presentation type should be labelled as Graph, Figure, or Table, and its sequence should be in running order, separate from each other.

Equations should be aligned to the left, and numbered with in running order with its number in parenthesis (aligned right).

Ⅻ. Others

Conflicts of interest, acknowledgements, and publication ethics should also be declared in the final version of the manuscript. Instructions have been provided as its counterpart under Cover Letter.

About the Publisher

Bilingual Publishing Co. (BPC) is an international publisher of online, open access and scholarly peer-reviewed journals covering a wide range of academic disciplines including science, technology, medicine, engineering, education and social science. Reflecting the latest research from a broad sweep of subjects, our content is accessible world-wide——both in print and online.

BPC aims to provide an analytics as well as platform for information exchange and discussion that help organizations and professionals in advancing society for the betterment of mankind. BPC hopes to be indexed by well-known databases in order to expand its reach to the science community, and eventually grow to be a reputable publisher recognized by scholars and researchers around the world.

BPC adopts the Open Journal Systems, see on ojs.bilpublishing.com

Database Inclusion

Asia & Pacific Science Citation Index

Creative Commons

China National Knowledge Infrastructure

Google Scholar

Crossref

MyScienceWork

BILINGUAL
PUBLISHING CO.
Pioneer of Global Academics Since 1984

Tel:+65 65881289
E-mail:contact@bilpublishing.com
Website:www.bilpublishing.com